RSC Advances

Controllable gold nanoparticles deposition on carbon nanotubes and their application in immunosensing

Journal:	*RSC Advances*
Manuscript ID:	RA-ART-04-2015-007990.R2
Article Type:	Paper
Date Submitted by the Author:	12-May-2015

Complete List of Authors:	Das, Ritu; DRDE, Biosensor Division Upadhyay, S.; Defence Research and Development Establishment (DRDE), Biosensor Division Sharma, Mukesh; DRDE, Biosensor Division Shaik, M; DRDE, Biosensor Division Rao, V; DRDE, Biosensor Division Srivastava, Divesh; Central Salt & Marine Chemicals Research Institute, Analytical Discipline & Centralized Instrument Facility

Controllable gold nanoparticles deposition on carbon nanotubes and their application in immunosensing

Ritu Das[a], Sanjay Upadhyay[a*] Mukesh K. Sharma[a], M.Shaik[a], V.K.Rao[a] and Divesh N.Srivastava[b]

Received (in XXX, XXX) Xth XXXXXXXXX 20XX, Accepted Xth XXXXXXXXX 20XX
DOI: 10.1039/b000000x

A CNT-AuNPs hybrid nanocomposite platform was prepared from nanodispersed AuNPs in *N*-[3-(trimethoxysilyl) propyl] ethylenediamine (EDAS) sol-gel matrices with purified MWCNT. EDAS, an amine group containing sol–gel solution utilizes its affinity for stabilizing the nanoparticles in solution. The developed model system was based on immobilized rabbit anti-mouse IgG-HRP (horseradish peroxidase) for reagentless detection of mouse IgG. The immunosensing platform was prepared by using nafion for the immobilisation of rabbit anti-mouse IgG-HRP (horseradish peroxidase) and CNT-AuNPs hybrid nanocomposite on glassy carbon electrode (GC) used for the detection of mouse IgG which provides a biocompatible microenvironment. The resulting CNT-AuNPs nanocomposite brings new capabilities for electrochemical devices by using the synergistic action of their electrocatalytic activity. The CNT-AuNPs were characterized using SEM, TEM, EIS, AFM and the analytical performance was monitored by differential pulse voltammetry. The detection limit of mouse IgG is 0.5 ng/mL(S/N ratio = 3). In addition, the immunosensor efficiently showed a specific electrochemical analysis of mouse IgG and easy discrimination with goat IgG, chicken IgG, and rabbit IgG.

Introduction

Carbon nanotubes (CNTs) have been widely explored for the development of analytical tools for diagnostic purposes, environmental analysis and food industries. It possesses the excellent property of high surface area, high electrical conductivity, good chemical stability and biocompatibility. These properties lead CNTs for the development of hybrid nanomaterials. Hence, extensive researches have been carried out on CNTs and their composites with noble metal nanoparticles (gold, platinum, etc.). CNTs and metal nanoparticles (MNPs) hybrid materials have attracted significant attention because of their unusual size-dependent electrical, chemical, and optical properties. CNT hybrid materials find a wide range of applications in areas such as electrocatalysis, nanoelectronics, medical diagnostics, biosensors, dehydrogenation catalysts and biological imaging [1-9]. All these applications lead to the requirement of synthesis of the vital structure of CNT-nanohybrid material without compromising the integrity of the underlying CNT framework. The properties of MNPs depend on the particle size dimensions, shape, synthesis route and its stability in aqueous/non-aqueous solution. Hence, the control of physical dimensions and size distribution of the nanoparticles on CNT surfaces are important parameters in the synthesis of the hybrid materials. The hydrophobic surface of CNT generally functionalized utilizing three main strategies to attach the nanoparticles or biomolecules for sensing purposes. It broadly classified as covalent approaches, non-covalent approaches and direct formation specifically used for AuNPs deposition on CNT[10]. The most-commonly used method is the covalent attachment of chemical groups such as carbonyl or carboxylic acid via acid treatment, CNTs functionalized by such approaches extensively oxidizes them by strong acid treatments to form COOH-functionalized CNTs. However, COOH-functionalized CNTs loses intrinsic properties due to damage to the π-conjugated CNT structure. Direct formation method formulates un-capped AuNP without any stabilizing monolayer ligand the CNTs using different approaches such as chemical vapour deposition, electrodeposition, and thermal decomposition. Limitation of this approach is need of complex instrumentation, slow deposition rate, and uneven size distribution of AuNPs. Furthermore, AuNPs fabricated in this fashion are unstable and undergo agglomeration. The non-covalent adsorption utilizes hydrophobic[11], π-π stacking[12], electrostatic[13], van der Waals interactions[14] between the native or treated CNT and the monolayer protected AuNPs. The significance of this approach is that it does not hamper the integrity of the chemical structure of the CNT sidewalls[15-26]. AuNPs have recognized as a versatile and effective label for the conjugation of biomolecules due to their rapid and simple chemical synthesis, a narrow size distribution and efficient coating of thiols and other bio-ligands. Colloidal AuNPs extensively used as an immobilization matrix as it provides a suitable microenvironment for retaining the bioactivity of macromolecules such as enzymes, proteins, antibodies, nucleic acid and promotes the direct electron transport between the active centre of the immobilized proteins[17]. However, the deposition of nanodisperse AuNPs on CNT has been extensively investigated, but still requires tedious procedures or instruments.

Embedding of various nanoparticles within sol-gel based matrices has a wide range of applicability[27-30]. Sol-gel process emerged as a promising method which can be carried out at low temperature, it is chemically inert in nature, has a porous structure, also posse's high-thermal stability, and has a wide potential window. Due to these facts, it considered as a matrix for encapsulating nanoparticles, immobilization of biomolecules and can easily cast in a variety of forms including monolith and thin films[31]. The aminosilane can also play a key role in the stabilization of nanoparticles in aqueous solution. Here, the Si-OH and the $-NH_2$ groups stabilizes the nanoparticles while the presence of only one of these functional groups is not enough to

complete the task [32, 33]. Considering the advantages of sol-gel technology as a matrix and providing the long term stability to nanoparticles, we have utilized it for the synthesis of nanodispersed AuNPs in sol-gel matrices by varying the composition of EDAS/water. In this nanodispersed AuNPs sol solution, purified MWCNT was mixed along with ethanol that reduces the interfacial tension between AuNPs sol solution and MWCNT. This MWCNT-AuNPs hybrid nanocomposites has used in immunosensing of IgG [34].

Electrochemical immunosensors have been widely used in the fields of clinical diagnosis, environmental analysis and food industry due to their precise, sensitive measurements, fast response time, the inherent simplicity, and miniaturization [34-40]. To improve the sensitivity of immunosensors various nanomaterials such as quantum dots, CNTs, graphene, magnetic beads, silica nanoparticles have been used [38-49]. Among the various hybrid nanomaterials, CNT-AuNPs have used widely for immunoassays [38-39,43,44]. AuNPs act as an immobilization support for retaining the bioactivity of biomolecules such as enzymes, proteins, antibodies [17, 50-52] and CNT provide excellent electrical conductivity and also help in immobilizing the biomolecules. The present approach implies the non-covalent interaction of AuNPs with CNT without hampering the integrity of the CNTs and the detection scheme is based on reagentless biosensor monitoring the direct electrochemistry of HRP in an immunoconjugated complex immobilized on the electrode surface.

In this study, we have developed a CNT-AuNPs hybrid nanocomposite by a simple and stable method using nanodispersed AuNPs in EDAS sol-gel matrix. AuNPs containing sol mixed with purified MWCNT along with ethanol that lowers the interfacial tension between AuNPs sol solution and MWCNT and used in immunosensing. By using sol-gel process for AuNPs synthesis it expected to lead control size and proper distribution of the AuNPs on CNT. The immunosensing platform has been constructed on glassy carbon electrodes (GC), and rabbit anti mouse IgG-HRP (horseradish peroxidase) along with CNT-AuNPs hybrid nanocomposite were immobilized in nafion matrix on GC electrode (nafion/CNT-AuNPs/Ab-HRP) for the detection of mouse IgG without using any other cross linking reagent. Present work is motivated by the promising results of hybrid nanomaterial for signal amplification and sensitive detection of the target molecule. This hybrid material provides direct electrical communication between redox sites of labelled enzymes (HRP) and the sensing surface eliminating the substrate addition. The electrochemical behaviour and other factors influencing the performance of the immunosensors have also been studied.

Materials and Methods

2.1 Materials and reagents

N-[3-(trimethoxysilyl)propyl]ethylenediamine (EDAS), MWCNT (90%), Nafion (perfluorinate 5 wt% solution), $NaBH_4$, rabbit anti mouse IgG-HRP, mouse IgG, chicken IgG, goat IgG, rabbit IgG, and human serum (minus IgA/IgM/IgG) were obtained from Sigma-Aldrich (St. Louis, U.S.A.). Gold (III) chloride trihydrate ($HAuCl_4.3H_2O$), potassium ferrocyanide [$K_4Fe(CN)_6.3H_2O$], potassium ferricyanide [$K_3Fe(CN)_6$]and hydrogen peroxide (30% H_2O_2) were purchased from Sigma-Aldrich Chemie GmbH (Steinheim, Germany) All other chemicals and reagents were of analytical grade. Aqueous solutions were prepared with double distilled water.

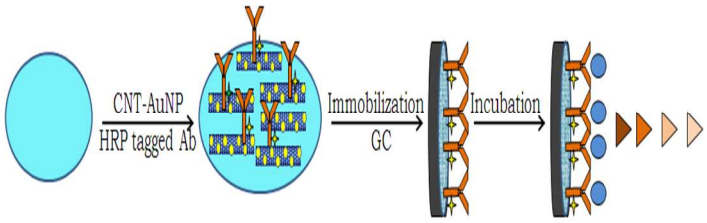

Scheme 1 Schematic representation of fabrication of immunosensor

2.2 Apparatus

The electrochemical measurements were performed on a PGSTAT 12 potentiostat obtained from Autolab with GPES software (EcoChemie). A conventional three-electrode system comprising glassy carbon electrode (dia. = 2 mm) as the working electrode after modification with CNT-AuNPs with rabbit anti mouse IgG-HRP (horseradish peroxidase) in nafion matrix, platinum wire as auxiliary electrode and Ag/AgCl electrode as a reference electrode were used for electrochemical studies. Differential pulse voltammetry measurements were performed in 0.1 M phosphate buffer (pH 7.4). All experiments were performed at room temperature (25±1°C). The TEM imaging was done using a JEOL JEM 2100 microscope at 200 kV acceleration voltage. The sample was dispersed in ethanol and loaded over lacey carbon coated copper TEM grid (300 mesh). The solvent was evaporated under the ambient room conditions before loading the sample into the machine.

2.3 Preparation of integrated silicate-Au nanoparticles architecture

The EDAS sol was prepared by adding 1 ml EDAS (97%) solution to 8.5 ml water and 0.5 ml HCl (0.1 M) (for hydrolysis and condensation) under continuous stirring for 2h. 1 ml of 1 mM $HAuCl_4$ was added in 9.0 mL EDAS sol solution and sonicated for 10 min, a clear yellow solution was obtained. The solution was reduced by adding 0.05mL of a freshly made 5% $NaBH_4$ solution with constant stirring and change in color was observed from yellow to deep wine red. This solution was stirred for 30 min for better homogeneity.

2.4 Preparation of AuNPs decorated MWCNTs

The purified MWCNT (1mg) was dispersed in 2ml EDAS-AuNPs sol and sonicated for 1 h to obtain a homogeneous suspension. From this EDAS-AuNPs-MWCNT suspension, 1ml suspension was mixed with 500 µl of ethanol followed by sonication for 1h and stirring for 5 h simultaneously. Afterwards, the resulting mixture was centrifuged, and the pellet obtained containing AuNPs-MWCNT composite was washed repeatedly with distilled water and suspended in 1% nafion solution (Nafion/CNT-AuNPs).

2.5 Fabrication of immunosensors

Prior to immobilization of rabbit anti mouse IgG-HRP, the GC electrode was polished before each experiment with 0.3 and 0.05

µm alumina powder then sequentially sonicated in HNO_3, ethanol and distilled water and dried at room temperature. One microliter of HRP tagged rabbit anti-mouse IgG mixed with five microliters of nafion/CNT-AuNPs and dropped on the precleaned GC electrode surface (scheme 1). The electrode dried under ambient condition and was stored at 4°C when not in use.

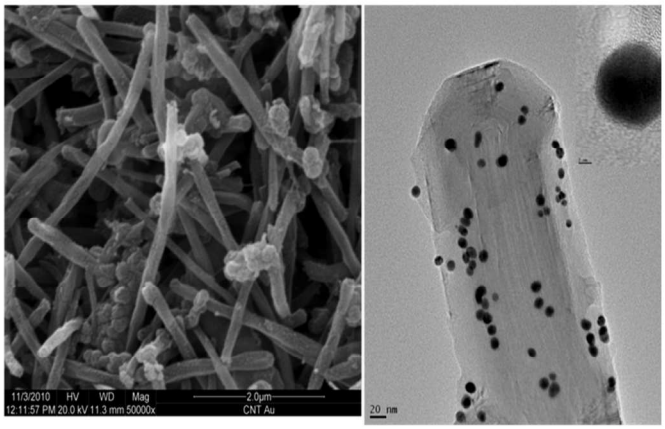

Fig 1(a) SEM image and (b) TEM image of CNT-AuNPs hybrid nanocomposite (inset shows the single AuNP).

2.6 Electrochemical assay

The prepared immunosensor was incubated in phosphate buffer (pH 7.4) containing mouse IgG of different concentration at 37°C for 30 min to form the immunocomplex and then rinsed carefully with PBS buffer. The cyclic voltammetry and differential pulse voltammogram measurements were performed to study the direct electrochemistry of the immobilized HRP in phosphate buffer (pH 7.4) which was deareated thoroughly with nitrogen gas for 15 min. The same method was used for the specificity studies using different IgG.

3. Results and discussion

3.1 Morphology of CNT-AuNPs modified electrode

SEM and TEM images of CNT-AuNPs are presented in Fig. 1a & b respectively. The AuNPs have a proper distribution on the CNT surface and can be considered as nanoparticle hybrid nanodispersed ensemble. Fig. 1a shows the SEM morphology of the CNT-AuNPs. The high aspect ratio interpenetrating carbon nanotubes can be observed in this figure, the coating of AuNPs cannot be observed the SEM image, and however the magnified TEM image of the composite in Fig. 1b displays the AuNPs coated CNT. The average size of the AuNPs was measured to be around 6-10 nm and each are nearly spherical in shape (Fig 1b). The proper distribution of gold nanoparticles on the tip and sidewalls of MWCNT was observed in the TEM image. The stability of the AuNPs in EDAS sol is very high, and no aggregation was observed after three months (Monitored the absorption band at λ_{max} = 520nm by UV-vis spectroscopy after fifteen days of interval continuously for three months) [24]. Here, the amphiphilic nature of ethanol reduced the interfacial tension between MWCNT and AuNP sol solution [23, 53, 54]. When EDAS-AuNPs-MWCNT suspension was mixed with ethanol (in section 2.4), the MWCNT was easily dispersed under ultrasonication resulting in proper distribution of gold nanoparticles on the surface of MWCNT.

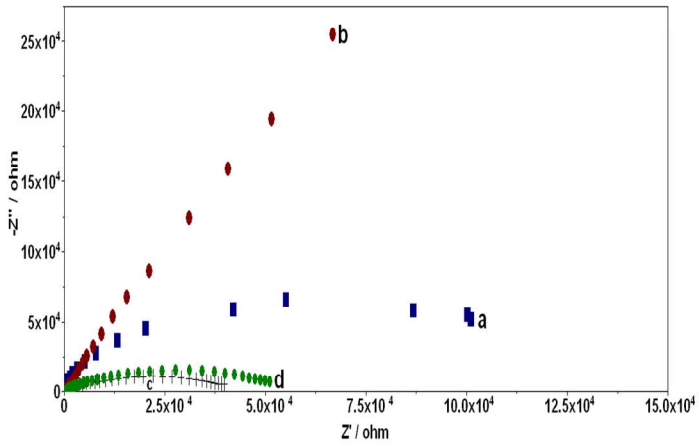

Fig 2 Nyquist plot in 1.0 mM $Fe(CN)_6^{-3/4-}$ containing 0.1 M KCl of different modified GC electrode (a) nafion modified GC electrode, (b) nafion/CNT-AuNPs on GC electrode, (c) nafion/CNT-AuNPs and HRP tagged rabbit antimouse IgG (nafion/CNT-AuNPs/Ab-HRP), (d) Immunoconjugate is formed after interaction with mouse IgG on CNT-AuNPs and HRP tagged rabbit antimouse IgG modified GC electrode.

3.2 Electrochemical behaviours of modified electrode

Electrochemical impedance spectra (EIS) was an effective method to study the electron transfer resistance at the electrode surface and interface properties of surface modified electrodes. Therefore it was employed to study the surface of the modified electrode with CNT-AuNPs and antigen antibodies interaction in 5mM $[Fe(CN)_6]^{3-/4-}$ containing 0.1 M KCl (Fig 2). Nyquist plots were plotted with a frequency range of 0.01 Hz to 10 kHz. The amplitude of the applied potential was set at 0.2 V. As shown in Fig 2 (curve a) 1% nafion modified electrode, the electron transfer resistance (Ret) was obtained ~110 KΩ suggesting that 1% nafion layer hinders the redox probe to the electrode surface. The introduction of CNT-AuNPs leads to significant decrease in the Ret value (Fig 2, curve b) which ascribed to high electron conduction pathways between the electrode and electrolyte due to CNT-AuNPs nanocomposite making easier to electron transfer to take place. When modified with CNT-AuNPs and HRP tagged rabbit antimouse IgG the Ret value increases, indicating HRP tagged antimouse IgG layer has immobilized on the surface and this bio-macromolecule layer obstructs the electron transfer (Fig 2, curve c). Subsequently, when immunoconjugate was formed on the electrode after interaction with mouse IgG the Ret value further increased (Fig 2, curve d) which was consistent with the fact of immunocomplex formation on the electrode surface insulating the conductive support and bound the interfacial electron transfer. These results indicate the effect of CNT-AuNPs nanocomposite as well as formation of immunocomplex on the electrode surface.

3.3 AFM image of the electrode after immobilization of antibodies and immunocomplex formation

Fig. S1(a) shows AFM image of CNT-AuNPs and HRP tagged a rabbit antimouse IgG on electrode, the topographical image shows the immobilization of antibodies with CNT-AuNPs nanocomposite. It covers the whole surface of the electrode, and their Z-scale height is ~ 110 nm. After incubation with mouse IgG immunocomplex is formed on the electrode

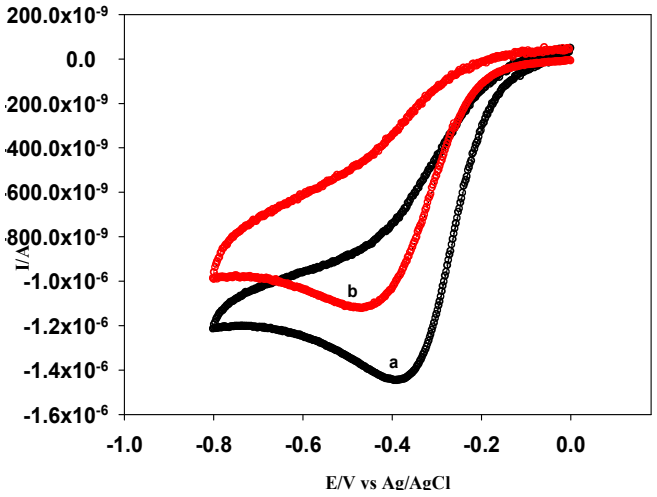

Fig 3. Cyclic voltammograms in 0.1 M phosphate buffer (pH 7.4) 0.1 M KCl at 10 mV/s of different modified GC electrode: nafion/CNT-AuNPs and HRP tagged rabbit antimouse IgG (nafion/CNT-AuNPs/Ab-HRP) on GC electrode without incubation with mouse IgG antigen (curve a), and after interaction with mouse IgG 0.5µg/mL on CNT-AuNPs and HRP tagged rabbit antimouse IgG modified GC electrode (curve b).

surface, AFM image clearly indicates a change in morphology of the electrode and its Z-scale height is ~ 220 nm (Fig S1 b). It confirms that immunocomplex is formed on the electrode surface that changes it morphology and increase in height is observed as compare with to Fig S1 (a).

3.4 Optimization of parameters for immunosensing

The incubation temperature and pH value of the solution both influenced the immunoreaction to achieve the sensitivity and reproducibility of the biosensor. Fig S2 (a) shows the effect of incubation temperature of antigen-antibody interaction (immunoreactions) on the modified electrode. The immunoreaction was monitored at different temperatures 25, 30, 34, 36, 37, & 40 °C, as the increase in incubation temperature the DPV response current decreases, which is favorable for immunocomplex formation. This immunocomplex increases the barrier of electron transfer between immobilized HRP tagged rabbit antimouse IgG and sensing surface, thus reducing the DPV current response. While at 37 °C the DPV current response became almost stable and further again increased with the increase in temperature. These results are consistent with a changing orientation of the immunocomplex on the surface of the electrode. At the incubation temperature of 37°C the DPV current response reached a stable value after 30 min (Fig. S2 a), indicating the saturated form of immunocomplex in the immobilized matrix. The optimal conditions for immunoreaction incubation are for 30 min at 37 °C. The effect of pH on the immunoreaction was explored between 5.0-8.0 in phosphate buffer solution. As shown in Fig S2 b, the current response decreases from pH 5.0 to 7.4 and reached to stability at pH 7.4. A further increase in buffer pH from 7.4 to 8.0 led to an increment of response. This is due to the influence of pH, at low and high pH the bioactivity of HRP tagged IgG will decline, which may be caused by denaturation of the immunocomplex, leading to an increase in the response current. Therefore, pH 7.4 was used to obtain the maximum electrocatalytic activity of the immobilized HRP tagged IgG for immunocomplex formation.

3.5 Analytical performance of the immunosensor

Immunosensor towards mouse IgG under optimized condition was investigated. Before performing DPV, we have

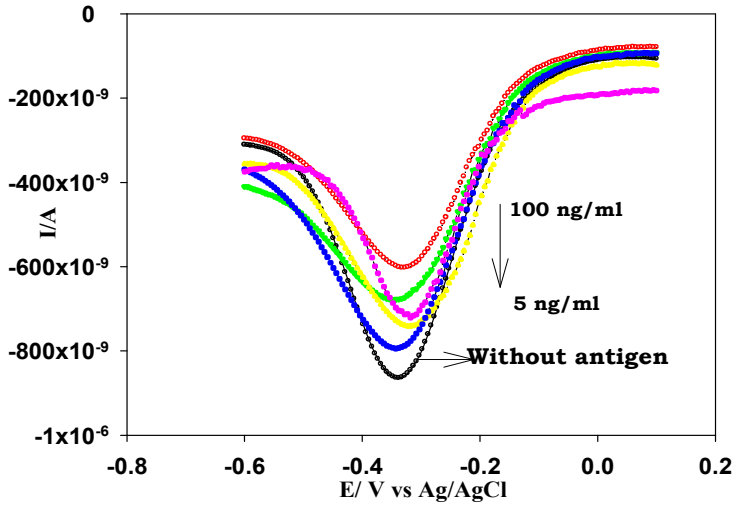

Fig. 4 (a) DPV of the immunosensor in 0.1 M phosphate buffer (pH 7.4) 0.1 M KCl after interaction with different concentrations of mouse IgG.

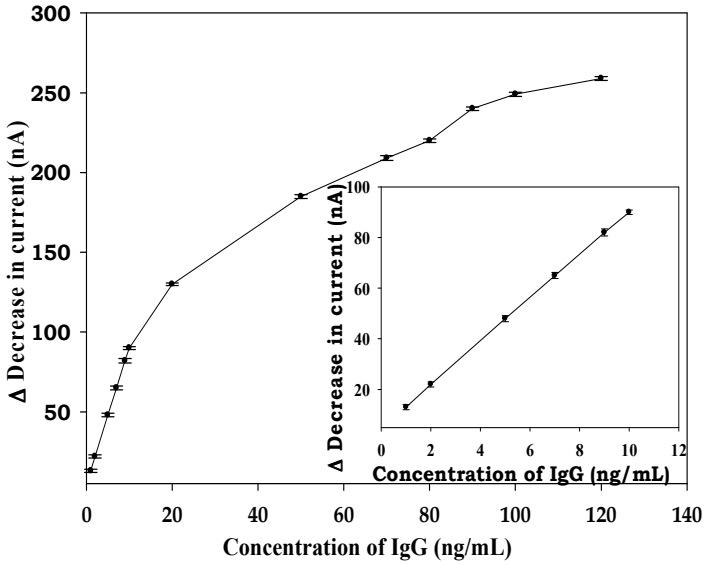

Fig. 4 (b). Calibration plot of decrease in DPV peak current vs mouse IgG concentration (n=3). Insets show linear calibration curve at lower range (1.0 to 10 .0 ng/mL).

monitored the cyclic voltammetry (CV) of the nafion/CNT-AuNPs modified electrode without HRP tagged antibodies (Ab-HRP) and nafion/CNT-AuNPs/Ab-HRP (data not shown). A very small peak (negligible) was observed at -0.58 V vs Ag/AgCl in nafion/CNT-AuNPs modified electrode (without HRP). The quasi-reversible peak was observed in nafion/CNT-AuNPs/Ab-HRP (with HRP). The peak was attributed to the redox active center of the HRP on the electrode surface. It ascribes the role of CNT-AuNPs in direct electron transfer between immobilized HRP tagged antibody and the electrode surface and also suggests the nafion/CNT-AuNPs as a favourable microenvironment for biomolecules immobilisation. Further, the CV of the nafion/CNT-AuNPs/Ab-HRP modified electrode in phosphate buffer (pH 7.4) was recorded in the absence of antigen and a peak was observed at -0.36 V vs Ag/AgCl (Fig 3 curve a). It is due to direct electron transfer between immobilized HRP tagged antibody and the electrode surface. Direct electron transfer between immobilized HRP and CNT-AuNPs and other nanomaterials has previously been reported by other researchers [38,39,41,46,53,54]. To achieve this goal, the immobilisation matrix has to be properly designed to allow protein to retain their native structure. Here, CNT-AuNPs served as a platform for both immobilization of biomolecules and direct electrical communication between redox sites of the enzyme label (HRP) and the sensing surface to avoid the substrate addition. In Fig 3, when immunosensor was incubated with mouse IgG (0.5 µg/mL) a gradual decrease in CV current was observed (Fig 3 curve b) due to the formation of immunocomplex. This decrease in current is attributed to the conformational restrictions of the HRP enzyme on the electrode surface for direct electron transfer on increasing the concentration of IgG, which hinders the electron transfer tunnel between immobilized HRP enzyme and the electrode surface. The decrease of CV current is proportional to the concentration of mouse IgG. Similarly, a concentration dependent decrease in

Table 1: Performance compared with reported immunosensors.

System	Target protein	Detection method	Detection limit	Reference
Hyd–MWCNT(AuNP)–Ab	Neomycin	Chronoamperometric	6.76 ng/mL	37
HRP-anti HCG/Au NP SG	hCG	DPV	0.3 mIU/mL	38
HRP-anti-CEA/NGGNs (nanogold enwrapped graphene)	CEA	CV	0.01ng/mL	47
Barium strontium titanate (BST)	hIgG	Impedance spectroscopy	40 ng/mL	48
anti-MIgG/NGs/TMB/Nf/GCE	MIgG	CV	1.0 ng/mL	49
nafion/CNT-AuNPs/Ab-HRP	Mouse IgG	DPV	0.5 ng/mL	Present work

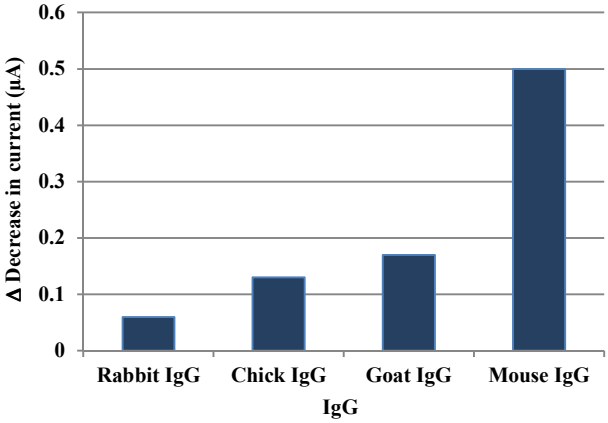

Fig. 5. Bar graph of decrease in DPV peak current response vs specificity of the immunosensor after interaction with different antigens of same concentartion 0.1μg/ml (a) mouse IgG, (b) chicken IgG, (c) rabbit IgG and (d) goat IgG

peak current was observed in the DPV measurements. Therefore, DPV was applied for sensing purposes (Fig 4 a). The decrease of DPV peak current is proportional to the concentrations of mouse IgG in the range from 5.0 to 100.0 ng/mL. The slight deviation in the peak potential was observed because of the response monitored on different electrodes. The relative standard deviations of the interelectrode variation was observed 5%.The corresponding calibration plot of decrease in DPV peak current versus mouse IgG concentration is shown in Fig 4 b. With the increasing concentration of mouse IgG two linear ranges can be discriminated; one from 1.0 to 10 ng/mL the other from 20-80 ng/mL at 3σ level. Almost the saturated current showed after 80 ng/mL to 120 ng/mL. The inset of Fig 4 b shows the lower range of the linear curve from 1.0 to 10 ng/mL. The detection limit of mouse IgG on CNT-AuNPs modified electrode corresponding to three times the standard deviation of the blank solution is estimated is around 0.5 ng/mL (S/N ratio 3.0) on CNT-AuNPs modified electrode. In Table 1 the performance of the present work compared with reported immunosensors. The present strategy demonstrates a sensitive detection when compared with other immunosensors except in[47] where the nanogold enwrapped with grapheme platform was used for detection of CEA.

3.6 Specificity of the immunosensor

One of the most important analytical factors for an immunosensor is the ability of the sensor to discriminate the interfering species similar to the target analyte. Specificity of the immunosensor was assessed using possible interfering species IgG incubation solution containing 0.1μg/ml of goat IgG, chicken IgG, and rabbit IgG and compare with mouse IgG of the same concentration (Fig 5). To some extent decrease in DPV peak current was observed with chicken, goat and rabbit IgG. As expected in the case of a mouse IgG a significant decrease in current response was observed. DPV peak current response of BSA was similar to that of the blank (without antigen). It demonstrates that current immunoassay could respond to mouse IgG specifically.

Table 2: The result of Mouse IgG detection in serum samples.

Sample number	Mouse IgG added (ng/mL)	Detected amount of Mouse IgG (ng/mL)	Recovery (%)
1	2.0	1.89	94.5
2	5.0	5.21	104.2
3	10.0	11.1	111.0
4	15.0	14.8	98.6
5	20.0	20.2	101.0
6	25.0	25.1	100.4

a

3.7 Reproducibility and stability of the immunosensor

The reproducibility of the immunosensors was confirmed by preparing four electrodes and monitoring the DPV response for 10 ng/mL of mouse IgG. All electrodes showed almost the same value of peak current. The reproducibility for four electrodes gave relative standard deviations of 6.4% for the determination of 10 ng/mL of mouse IgG. The good reproducibility observed due to presence of CNT-AuNPs nanocomposite with Ab-HRP on the surface of the electrode without losing its activity.

The stability of the immunosensor was evaluated over a period of one month at 4° C. The DPV response was monitored in each week (up to four weeks). The immunosensor response current maintained 97.2%, 94.7%, 93.5% and 92.2% of the initial response in each week respectively. It showed that the immunosensor had good storage stability.

3.8 Analysis of IgG in serum samples

In order to investigate the feasibility of immunosensor for real sample analysis, different concentrations of mouse IgG were added in the serum samples and analyzed by DPV method. The result showed that the recovery of mouse IgG from the serum samples was 94.5 to 111.0 % (Table 2). The relative standard deviations were less than 8.0% (n=3). The immunosensor showed that recovery from serum samples was good, and it has a potential analytical application for real sample analysis.

4. Conclusions

We have synthesized nanodispersed gold nanoparticles (AuNPs) by sol gel process and prepared CNT-AuNPs composites and with proper distribution of AuNPs on the tip and sidewalls of MWCNT. This CNT-AuNPs nanocomposite was employed for the construction of an immunosensor on a GC electrode (nafion/CNT-AuNPs/Ab-HRP) for the detection of mouse IgG. This nanocomposite effectively facilitates the direct electrical communication between redox sites of HRP labelled IgG and sensing surface to avoid the substrate addition. We have characterized the modified electrode with SEM, TEM, EIS and AFM and found that Ab-HRP was immobilized on the surface of CNT-AuNPs nanocomposite modified electrodes. The analytical performance of the immunosensor was studied, and a detection limit achieved up to 0.5 ng/mL mouse IgG was obtained (S/N ratio = 3). Furthermore, the specificity of the prepared immunosensor was also evaluated, and it showed good specificity towards mouse IgG with easy discrimination between goat IgG, chicken IgG, and rabbit IgG. The proposed immunosensor showed good reproducibility and stability for the detection of mouse IgG. The developed immunosensor on the CNT-AuNPs nanocomposite surface provided conspicuously enhanced electrochemical signals and this platform can be easily extended for other protein detection.

Notes and references

[a]*Defence Research and Development Establishment, Jhansi Road Gwalior-474002, INDIA*
[b] *Analytical Discipline & Centralized Instrument Facility*
CSIR-Central Salt & Marine Chemicals Research Institute Gijubhai Badheka Marg, Bhavnagar – 364021, India
Corresponding author: Sanjay Upadhyay
Email address: sanjayupad@rediffmail.com and sanjayupad@drde.drdo.in
Phone: + 91-751-2231859 Fax: +91-751-2341148

† Electronic Supplementary Information (ESI) available: [details of any supplementary information available should be included here]. See DOI: 10.1039/b000000x/

‡ Footnotes should appear here. These might include comments relevant to but not central to the matter under discussion, limited experimental and spectral data, and crystallographic data.

References

1. D. Eder, *Chem Rev.*, 2010, **110**, 1348-1385.
2. A. Yu, Z. Liang, J. Cho, F. Caruso, *Nano Letters*, 2003, **3**, 1203-1207.
3. J. Wang, *The Analyst*,. 2005, **130**, 421-426.
4 X. Luo, A. Morrin, A. J. Killard, M. R. Smyth, *Electroanalysis*, 2006, **18**, 319-326.
5 E. Katz, I. Willner, *Angw. Chem. Int. Ed*., 2004, **43**, 6042-6108.
6 B. Wu, Y. Kuang, X. Zhang, J. Chen, *Nanotoday*., 2011, **6**, 75-90.
7 K. Scida, P.W. Stege, G. Haby, G. A. Messina, C. D. García, *Anal.Chim Acta*, 2011, **691**, 6-17
8 H.Yang, R.Yuan, Y.Chai, H.Su, Y.Zhuo, W.Jiang, Z.Song, *Electrochimica Acta*, 2011, **56**, 1973-1980.
9 L.Jiang, J.H., F. Li, J.Gao, Y.Li, Y.Dong, Q.Wei, *Electrochimica Acta*, 2015, **160**, 7-14.
10 R. Singh, T. Premkumar, J.Y. Shin, K.E. Geckeler, *Chemistry - A European Journal*, 2010, **16**, 1728–1743,
11A.V.Ellis , K.Vijayamohanan , R.Goswami , N.Chakrapani , L.S.Rama nathan , P. M.Ajayan , G.Ramanath, *Nano Letters*,2003, **3**, 279–282
12 L.Liu, T. Wang, J.Li, Z.X.Guo, L.Dai, D.Zhang, D.Zhu, *Chemical Physics Letters*, 2003, **367**, 747–752.
13 M.A. Herrero ,J. Guerra, V. S. Myers,M.V. Gomez, R.M.Crooks, M. Prato, *ACS Nano*, 2010, **4**, 905.
14 G.A.Rance, D.H.Marsh, S.J Bourne, T.J. Reade, A.N. Khlobystov, *ACS Nano*., 2010, **24**, 4920-8.
15 H.Ozawa, X.Yi, T.Fujigaya, Y.Niidome, T.Asano, N.Nakashima, *J.Am.Chem.Soc*., 2011, **133**, 14771-14777.
16 P.Salice, A.Gambarin, N.Daldosso, F.Mancin, E. Menna, *J.Phys.Chem*., 2014, **118**, 27028-27038
17 M.Daniel,D.Astruc, *Chem. Rev*., 2004, **104** 293.–346.
18 R. Y. Zhang, H. Olin, *Int. J. Biomedical Nanoscience and Nanotechnology*, 2011, **2**, 112-135.
19 Y. Xiao, H. Ju, H. Y. Chen, *Anal. Biochem*., 2000, **278**, 22-28.
20 Stolarczyk, D.Fitzmaurice, *J Phys Chem B*, 2005, **109**, 16310-163125.
21 D.Ragupathy, A.I. Gopalan, K.-P.Lee, *Electrochem. Commun*., 2009, **11**, 397-401.
22 G. Jeong, S. Suzuki,Y. Kobayashi, *Nanotechnology,* 2009, **20**, 285708.
23 Y. Shi, R.Yang, P.K.Yuet, *Carbon*, 2009, **47**, 1146-1151.
24 S.Y.Moon, T.Kusunose, S-I.Tanaka, T.Sekino, *Carbon*, 2009, **47**, 2924-2932.
25 E.Katz, I. Willner, J.Wang, *Electroanalysis*, 2004, **16**,19-44.
26 B.K. Jena, C.R. Raj, *Anal. Chem*., 2006, **78**, 6332–6339.
27 H. Chen, S. Dong, *Biosens. Bioelectron*., 2007, **22**, 1811–1815.
28 R.Szamocki, S. Reculusa, S.Ravaine, P.N.Bartlett, A.Kuhn, R.Hempelmann, *Ang Chem.Int.Ed.*, 2006, **45**, 1317-1321.
29 Y.Kobayashi, M.A.Correa-Duarte, L.M.Liz-Marzan**,** *Langmuir*, 2001, **17**, 6375-6379.
30 Y. Li, M.A. El-Sayed, *J. Phys. Chem. B*, 2001, **105**, 8938–8943.
31 S. Upadhyay, M. K. Sharma, G. R. Rao, B. K. Bhattacharya, V. K. Rao, R. Vijayaraghavan , *Analytical Methods*., 2011, **3**, 2246-2253.
32 H.C.Choi, M.Shim, S.Bangsaruntip, H.J.Dai, *J.Am.Chem.Soc.*, 2002, **124**, 9058-9059.
33 Y.Zhuo, W-J Yi, W-B Lian, R. Yuan, Y-Q Chai, A.Chen, C-M. Hu, *Biosens. Bioelectron*., 2011, **26**, 2188-2193.

34 S.C.B.Gopinath, T.-H.Tang , M. Citartan , Y. Chen , T. Lakshmipriya., *Biosens.Bioelectron*., 2014, **57**, 292-302.

35 F.Ricci, G.Adorenetto, G.Palleschi, *Electrichim Acta*, 2012, **84**, 74-83.

36 J.E.N.Dolatabadi, M.D.L. Guardia, *Analytical Methods*, 2014, **6**, 3891-3906.

37 Ye Zhu, Jung Ik Son, Yoon-Bo Shim, *Biosens.Bioelectron*., 2010, **26**, 1002-1008.

38 Jin Chen, Jinhai Tang, Feng Yan, Huangxian Ju, *Biomaterials*, 2007, **27**, 2313-2321.

39 Zhi-Da Gao, Fang- Fang Guan, Cheng-Yong Li, Hai-Feng Liu, Yan-Yan Song, *Biosens.Bioelectron*., 2013, **41**, 771-775.

40 Q.Wei, K.Mao, D.Wu, Y.Dai, J.Yang, B.Du, M.Yang, H.Li, *Sensors and Actutors B: Chemical*, 2010, **149**, 314-318.

41 R. Cui, H. Huang, Z. Yin, D. Gao, J.-J. Zhu, *Biosens.Bioelectron*., 2008, **23**, 1666-1673.

42 X.Gao, Y. Zhang, H. Chen, Z. Chen, X. Lin, *Anal. Biochem*., 2011, **414**, 70-76.

43 S.Mao, G.Lu, K. Yu, J.Chen, *Carbon*, 2010, **48**, 479-486.

44 H.Chen, C. Jiang, C.Yu, S.Zhang, B. Liu, J. Kong, *Biosens. Bioelectron.*, 2009, **24**, 3399-3411.

45 M. Dequarie, C.Degrand, B.Limoges, *Anal. Chem*., 2000, **72**, 5521-5528.

46Y. Xiao, H. Ju, H. Y. Chen, *Anal. Biochem*. 2000, **278**, 22-28.

47 Z. Zhonga, W. Wub, D. Wanga, D. Wangc, J. Shana, Y. Qinga, Z. Zhanga, *Biosens. Bioelectron*., 2010, **25**, 2379-2383.

48 X. Fang, O.K. Tan, Y. Y. Gan, M. S. Tse, *Sensors & Actuators B: Chemical,* 2010, **149**, 381-388.

49 Y.Wu, J. Zheng, Z.Li, Y. Zhao, Y. Zhang, *Biosens. Bioelectron*., 2009, **254**, 1389-1393.

50 X.Cao, Y.Ye, S.Liu, *Anal.Biochem.*, 2011, **417**, 1-16.

51 F.Reincke, S.G. Hickey, W.K.Kegel, D.Vanmaekelbergh, *Angew Chem Int Ed.,* 2004, **43**, 458-462.

52 P.Cheng, D.Li, Z.Yuan, Y. Zou, D.Yang, *Mater. Chem. Phys.,* 2008, **111**, 271-274.

53 J. Jia, B. Wang, A. Wu, G.Cheng, Z. Li, S. Dong, *Anal Chem*., 2002, **74**, 2217-2223.

54 G. K. Ahirwal, C. K. Mitra, *Sensors,* 2009, **9**, 881-894.

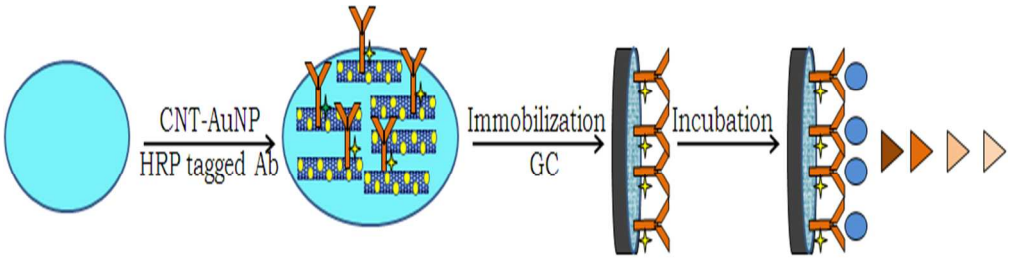

Scheme 1